Health Monitoring and Drift Detection of Bearing Using Direct Density Ratio Estimation

Sanjoy Kumar Saha¹, M.M. Manjurul Islam¹, Shaun McFadden¹, Mark Gorman², Saugat Bhattacharyya¹ and Girijesh Prasad¹

¹ Ulster University, Londonderry, Northern Ireland, BT48 7JL, United Kingdom saha-sk@ulster.ac.uk m.islam@ulster.ac.uk s.mcfadden2@ulster.ac.uk s.bhattacharyya@ulster.ac.uk g.prasad@ulster.ac.uk

² Seagate Technology, Londonderry, Northern Ireland, BT48 0BF, United Kingdom mark.gorman@seagate.com

ABSTRACT

Prognostics and health management (PHM) has been widely employed for condition monitoring, fault diagnosis and failure prediction in mechanical systems. However, the presence of uncertainty and transient fluctuations in condition monitoring data makes the precise detection of degradation challenging. This paper presents a novel direct density ratio estimation (DDRE) method that computes the change score of the health indicator to detect degradation. The approach continuously computes the change score between two sliding windows using noise-assisted relative unconstrained least-squares importance fitting (NA-RuLSIF). This study does not rely solely on magnitude of the DDRE-based dissimilarity score; instead, it analyses the dynamic behaviors of the change score to categorize degradations into steady and progressive types. Additionally, this research identifies the onset of runaway failures, referred to as the initial degradation point (IDP), which is used as the starting point for remaining useful life (RUL) estimation. To validate the proposed approach, a publicly available rollingelement bearing dataset is utilized. Experimental results demonstrate the effectiveness and robustness of the proposed DDRE method for both degradation detection and selection of the IDP.

1. Introduction

Predictive maintenance of rolling bearings has become prevalent among researchers because they are extensively used in many mechanical devices (Wang et al., 2020). The

Sanjoy Saha et al. This is an open-access article distributed under the terms of the Creative Commons Attribution 3.0 United States License, which permits unrestricted use, distribution, and reproduction in any medium, provided the original author and source are credited.

degradation of bearing health affects the performance and reliability of mechanical equipment. In industry, sudden failure of mechanical equipment causes production disruption (Bajarunas et al., 2024). Therefore, early detection of any kind of degradation and fault is necessary to implement fault-tolerant operation and to optimise maintenance schedules (Liang et al., 2018). In predictive maintenance, a condition-based approach is used to monitor the actual condition and to predict the remaining useful life (RUL) (Surucu et al., 2023). Using RUL, the maintenance schedule can be designed to minimize unplanned downtime of assets. However, many studies have focused on RUL prediction rather than degradation detection (Wang et al.,

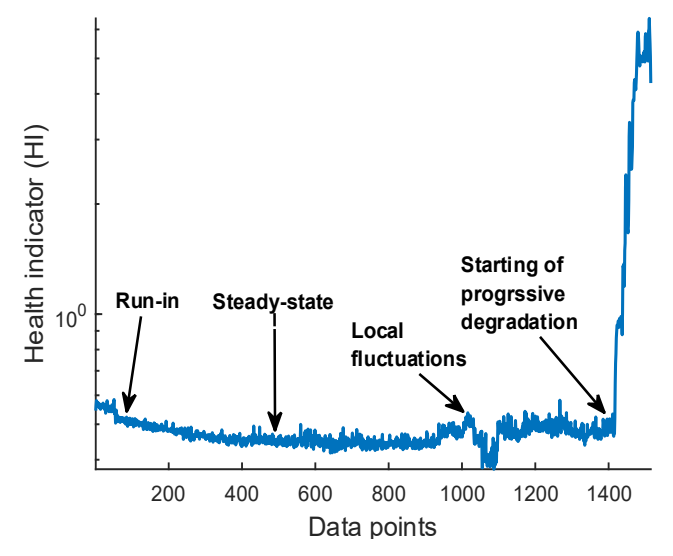


Figure 1. A typical rolling bearing life cycle with bearing health indicator (HI) on logarithmic scale.

2021). Additionally, accurate detection of the IDP is crucial for improving RUL prediction (Yang et al., 2025).

During continued operation of rotating machinery, rolling bearings undergo gradual degradation, transitioning from a normal health condition to a deteriorated state that may ultimately result in failure. Consequently, many studies divide the bearing life cycle based on condition-monitoring data into two distinct phases: (1) a normal phase and (2) an abnormal phase (Ahmad et al., 2018). The onset of the abnormal phase is defined as the initial degradation point (IDP) and is considered the optimal starting point for RUL estimation. However, in real world, bearings typically traverse multiple phases of degradation rather than a simple two-stage framework (Halme & Andersson, 2010). In the full life cycle of a bearing, three distinct phases are typically observed: (1) run-in, (2) steady-state operation, and (3) progressive degradation. The run-in phase is the initial stage of wear at the onset of service life, during which microscopic high spots on the rolling elements and raceways generate elevated vibration levels. After these asperities are polished off, the bearing enters the steady-state (or "normal") phase, characterized by low, stable vibration amplitudes. During longer operation, minor surface wear and lubricant-film settling induce a subtle baseline shift from that steady condition, although overall vibration remains quasi-stable. Finally, progressive degradation begins with the formation of microscopic defects, which propagate over time, leading to a continuous increase in vibration levels until failure occurs (Patel & Patel, 2024). Additionally, bearing health can be affected by sudden geometric misalignment, lubricant contamination with wear particles, micro-pitting, and inadequate lubrication, all of which introduce local fluctuations in the condition-monitoring data. Therefore, bearings condition monitoring data exhibit multiple stages and variabilities. Figure 1 illustrates different levels of degradation a bearing undergoes during a run-to-failure scenario. As shown, in the figure, a single alarm level is not sufficient for handling both local fluctuations and progressive degradation.

Over the past decades, vibration-based condition monitoring has been the predominant approach for defect tracking. A range of time-frequency metrics, root-mean-square (RMS), kurtosis, crest factor, RMS-entropy estimator (RMS-EE), and frequency spectrum partition summation (FSPS) derived from vibration signals have been used as health indicators (HI) to track bearing degradation, as reported in the existing research (Lei et al., 2018; Minhas et al., 2021). Additionally, to address the non-stationarity of signals, empirical mode decomposition (EMD) and its variants, such as ensemble-EMD, wavelet packet decomposition (WPD) have been widely adopted to detect early-stage microcracks (Zhu et al., 2019). For IDP determination, only a limited number of existing studies are available. Recent works continue to employ subjective approaches for IDP detection (Gao et al., 2024). Additionally, a 3σ criterion-based technique, adopted from engineering standard ISO 10816, is very popular in this domain. Using this approach, an IDP is flagged based on exceedance of a predefined standard deviation (N. Li et al., 2015). Again, some researchers have proposed consecutive threshold exceedances for detection of IDP to solve the random noise in HI. A gradient-based linear regression model was proposed to select the IDP from RMS values (Ahmad et al., 2018). Furthermore, relying on a single threshold for diagnostics is inadequate for two primary reasons. First, a universal value cannot account for the operational variability across all bearings. Second, such a threshold is generally set high to prevent false alarms, which makes it insensitive to the subtle signs of an IDP and effective only in identifying severe degradation. Furthermore, a oneclass LSSVM-based approach for IDP detection was used by Islam et al. (2021). A risk assessment-based method was proposed to determine IDP via Mahalanobis distance fusion and CUMSUM techniques (Q. Li et al., 2022). Additionally, a two-stage IDP detection scheme was proposed by Cheng et al, (2022), which first applied a dynamic 2σ threshold principle based on continuous RMS exceedance. Subsequently, a nonparametric Mann-Kendall(M-K) test was employed to statistically verify the presence of a significant upward trend, effectively addressing transient fluctuations. Existing research on degradation detection has shortcomings understanding failure mechanisms and overall performance, which limits its real-life applicability. Moreover, a single alarm level is insufficient to handle both local fluctuations and progressive degradation.

For change detection, the Pearson divergence (PE) of HI, is commonly used, where individual densities of reference and test windows are calculated to find dissimilarity score using kernel density estimation (KDE). Subsequently, the ratio of the two computed densities is calculated to find the dissimilarities between samples. However, this approach introduces errors during individual KDE-based density estimations and is further amplified when the ratio is calculated. To overcome this issue, this research employs direct density ratio estimation (DDRE) by directly calculating the density ratio, thereby minimizing computational errors (Huang et al., 2006). Several methods exist for DDRE, such as kernel mean matching, unconstrained least-squares importance fitting(uLSIF) (Sugiyama et al., 2012) and relative uLSIF (RuLSIF) (Liu et al., 2013a). Among these, RuLSIF shows better performance for change detection. However, DDRE-based algorithms have not been utilized for applications in PHM.

The main purpose of this study is to identify and track the degradation using conventional HI. This study adopted the root means square (RMS) of vibration signals as HI because this metric captures better degradation stages of rolling bearings. A major challenge of RuLSIF algorithm is its sensitivity to local fluctuations in HI, which may sometimes be misinterpreted as changes or drifts. To address this problem, this study proposes a noise-assisted RuLSIF (NA-

RuLSIF) method. In this approach, two moving windows, named the reference and test windows, are used along with white noise to continuously calculate a change score. Afterward, sudden and progressive changes are automatically identified based on the height and width of the score peaks. The onset of runaway failure in the HI—referred to as the IDP—is identified as the starting point for RUL estimation. Despite abrupt temporary variations in HI, the proposed method performs precise identification of the IDP.

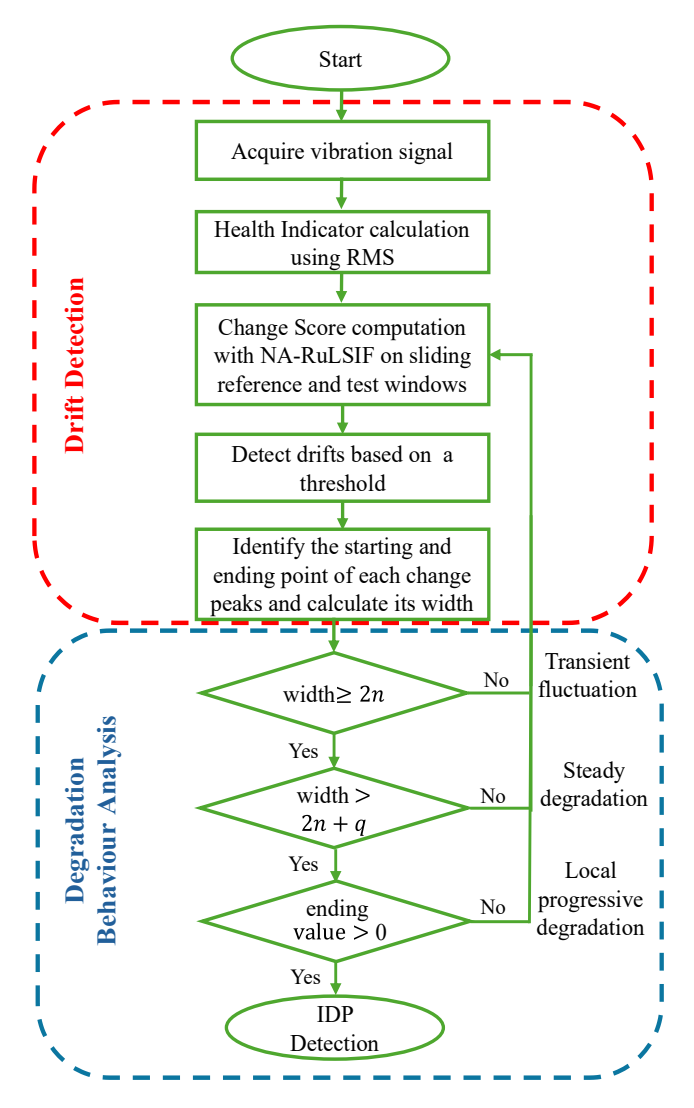


Figure 2. Flowchart of the proposed methodology for drift detection and classification of degradation patterns.

2. THEORETICAL BASIC: DIRECT DENSITY RATIO ESTIMATION FOR DRIFT DETECTION

In this section, the proposed framework for condition monitoring and drift detection of bearing health is discussed. Figure 2 illustrates the overall workflow of the framework. In the first stage, all kinds of drifts are detected and removed based-on change score computed by the NA-RuLSIF algorithm. In the next stage, each detected drift is categorized based on behavioral analysis of change score.

2.1. Problem Statement for Change Detection

For a given univariate time series, a sequence vector Z(t) is constructed at each time step t with previous k observations formally defined as:

$$Z(t) = \begin{bmatrix} z(t) \\ z(t-1) \\ \vdots \\ z(t-k+1) \end{bmatrix} \in \mathcal{R}^k$$
 (1)

To detect a change-point, the algorithm compares two distinct samples of sequences by $\mathcal{Z}_{test}(t)$ and $\mathcal{Z}_{ref}(t)$. Where a test sample, $\mathcal{Z}_{test}(t)$, consists of the n most recent sequences while reference sample $\mathcal{Z}_{ref}(t)$ comprise the preceding n sequences. These are defined as:

$$\begin{split} & \mathcal{Z}_{test}(t) = \{Z(t), Z(t-1), \dots, Z(t-n+1)\} \\ & \mathcal{Z}_{ref}(t-n) \\ & = \{Z(t-n), Z(t-n-1), \dots, Z(t-2n+1)\} \end{split} \tag{2}$$

The primary objective is to calculate a change score, CS(t), which quantifies the statistical distance between a test and the reference samples at time t-n, identified as the likely change-point. Under unchanged conditions both samples should be statistically similar. However, when a change occurs at t^* , their underlying distributions diverge.

Consider two underlying distributions $P_{test}(Z)$ and $P_{ref}(Z)$ for two sets of samples Z_{test} and Z_{ref} respectively. Now, α -relative Pearson (PE) divergence can be written as:

$$PE_{\alpha} := \frac{1}{2} \mathbb{E}_{P_{\alpha}(Z)} [(w_{\alpha}(Z) - 1)^{2}]$$
(3)

Here $w_{\alpha}(Z)$ is the α -relative density ratio of $P_{test}(Z)$ and $P_{ref}(Z)$ defined as:

$$w_{\alpha}(Z) := \frac{P_{test}(Z)}{P_{\alpha}(Z)}$$

$$w_{\alpha}(Z) := \frac{P_{test}(Z)}{\alpha P_{test}(Z) + (1 - \alpha) P_{ref}(Z)}$$
(4)

Again in Eq. (3), $\mathbb{E}_{P(Z)}[f(Z)]$ denotes the expectation of f(Z) under the distribution P(Z):

$$\mathbb{E}_{P(Z)}[f(Z)] = \int f(Z) P(Z) dZ$$

2.2. Direct Density Ratio Estimation

Let $\widehat{w}_{\alpha}(\mathcal{Z})$ be the estimated ratio modelled by a regression model. This model is fitted by minimizing the expected squared loss J as follows:

$$J = \frac{1}{2} \mathbb{E}_{P_{\alpha}(Z)} \left[\left(w_{\alpha}(Z) - \widehat{w_{\alpha}}(Z) \right)^{2} \right]$$

$$= \frac{1}{2} \mathbb{E}_{P_{\alpha}(Z)} \left[\left(\frac{P_{test}(Z)}{P_{\alpha}(Z)} \right)^{2} + \widehat{w_{\alpha}}(Z)^{2} \right]$$

$$- 2 \frac{P_{test}(Z)}{P_{\alpha}(Z)} \widehat{w_{\alpha}}(Z) \right]$$

$$= \frac{\alpha}{2} \mathbb{E}_{P_{test}(Z)} [\widehat{w_{\alpha}}(Z)^{2}] + \frac{1 - \alpha}{2} \mathbb{E}_{P_{ref}(Z)} [\widehat{w_{\alpha}}(Z)^{2}]$$

$$- \mathbb{E}_{P_{test}(Z)} [\widehat{w_{\alpha}}(Z)]$$

$$(5)$$

where the first term is constant and ignored during the minimization process. The density ratio is estimated with following kernel methods:

$$\widehat{w}_{\alpha}(\mathcal{Z}) \coloneqq \sum_{l=1}^{n} \theta_{l} \mathbb{K}(\mathcal{Z}, \mathcal{Z}_{l}) \tag{6}$$

where, parameters θ_i : = $(\theta_1, \theta_2, ..., \theta_p)$ to be learned from the data samples $\mathcal{Z}_{test}(t)$ and $\mathcal{Z}_{ref}(t-n)$. Again, $\mathbb{K}(\mathcal{Z}, \mathcal{Z}_i)$ is a kernel basis function and in this algorithm Gaussian kernel is used for change detection as:

$$\mathbb{K}(\mathcal{Z}, \mathcal{Z}_l) = exp\left(-\frac{\|\mathcal{Z} - \mathcal{Z}_l\|^2}{2\sigma^2}\right); \sigma > 0$$
 (7)

By substituting the approximating expectations from Eq. (5) with their empirical counterparts, the optimization problem can be written as follows:

$$\widehat{\theta} := \arg\min_{\theta \in \mathcal{R}^n} \left[\frac{1}{2} \theta^T \widehat{H} \theta - \widehat{h}^T \theta + \frac{\lambda}{2} \theta^T \theta \right]$$
 (8)

where a penalty term $\frac{\lambda}{2}\theta^T\theta$ is included for regularization purposes and λ (>=0) denote the regularization parameter. Here, we adopt the baseline of RuLSIF parameterization by selecting kernel width, $\sigma = 10^{-3}, 10^{-2}, \dots, 10^3$ and regularization parameter, $\lambda = 10^{-3}, 10^{-2}, \dots, 10^1$ (Liu et al., 2013b).

Furthermore, \widehat{H} is the $n \times n$ matrix with the (l, l')-th element.

$$\widehat{H}_{l,l'} =: \frac{\alpha}{n_{test}} \sum_{l=1}^{n_{test}} \mathbb{K}(Z_{test,l}, Z_{test,l}) \, \mathbb{K}(Z_{test,l}, Z_{test,l'})$$

$$+ \frac{1-\alpha}{n_{ref}} \sum_{j=1}^{n_{ref}} \mathbb{K}(Z_{ref,j}, Z_{ref,l}) \, \mathbb{K}(Z_{ref,j}, Z_{ref,l'})$$

$$(9)$$

and \hat{h} is an *n*-dimensional vector with *l*-th element define as,

$$\hat{h}_l =: \frac{1}{n_{test}} \sum_{i=1}^{n_{test}} \mathbb{K} \left(\mathcal{Z}_{test,i}, \mathcal{Z}_{test,l} \right)$$
(10)

Now it is easy to confirm that the solution of Eq. (8) can be analytically obtained as

$$\hat{\theta} = (\hat{H} + \lambda I_n)^{-1} \hat{h}. \tag{11}$$

2.3. Change Score Estimation Based on Noise Assisted-RuLSIF (NA-RuLSIF)

To evaluate the robustness of the proposed algorithm against measurement uncertainty and local fluctuation, additive white gaussian noise (AWGN), WN was introduced to the original Z_{test} and Z_{ref} as follows:

$$\begin{split} Z_{test}^{NA} &= \mathcal{Z}_{test} + (\beta \times WN) \\ Z_{ref}^{NA} &= \mathcal{Z}_{ref} + (\beta \times WN) \end{split} \tag{12}$$

where $WN \sim \mathcal{N}(0,1)$ and $\beta = 0.05$. Choosing β corresponds to noise with a standard deviation equal to 5% of a unit-variance Gaussian random variable. The use of a zero-mean distribution ensures that the noise does not introduce a systematic bias into the signal.

Using an estimated density ratio, $\widehat{w_{\alpha}}$ into Eq. (3), one obtains a closed-form estimator for the α -relative PE divergence after straightforward algebraic calculation described in (Yamada et al., 2013) and this divergence can be equivalently expressed as:

$$PE_{\alpha} = -\frac{\alpha}{2} \mathbb{E}_{P_{test}(Z^{NA})} [\widehat{w}_{\alpha}(Z^{NA})^{2}]$$

$$-\frac{(1-\alpha)}{2} \mathbb{E}_{P_{ref}(Z^{NA})} [\widehat{w}_{\alpha}(Z^{NA})^{2}]$$

$$+\mathbb{E}_{P_{test}(Z^{NA})} [\widehat{w}_{\alpha}(Z^{NA})] - \frac{1}{2}$$
(13)

Based on Eq. (13), each expectation is replaced by the corresponding sample average and obtained empirical estimator can be written as:

$$\widehat{PE}_{\alpha} = -\frac{\alpha}{2n_{test}} \sum_{i=1}^{n_{test}} \widehat{w}_{\alpha} (Z_i^{NA})^2
-\frac{(1-\alpha)}{2n_{ref}} \sum_{i=1}^{n_{ref}} \widehat{w}_{\alpha} (Z_i^{NA})^2
+\frac{1}{n_{test}} \sum_{i=1}^{n_{test}} \widehat{w}_{\alpha} (Z_i^{NA}) - \frac{1}{2}$$
(14)

here \widehat{PE}_{α} represents the estimated PE divergence from $P_{test}(Z^{NA})$ to $P_{ref}(Z^{NA})$ and equivalently, \widehat{PE}_{α} can be rewritten as $\widehat{PE}_{\alpha}(P_{test}(Z^{NA}) \parallel P_{ref}(Z^{NA}))$. Because PE divergence is not symmetric therefore change score D(t) can be defined by summing divergence in both directions as:

$$D(t) = \widehat{PE}_{\alpha} \left(P_{test}(Z^{NA}) \parallel P_{ref}(Z^{NA}) \right)$$

$$+ \widehat{PE}_{\alpha} \left(P_{ref}(Z^{NA}) \parallel P_{test}(Z^{NA}) \right)$$
(15)

2.4. Change Score Evaluation

In continuous change score, larger values of D(t) indicate that t - n is likely the true change-point. To evaluate change score, each timestamp t is labelled as:

$$\mathcal{L}(t) = \begin{cases} 1, & t^* \le t \le t^* + 2n \\ 0, & otherwise \end{cases}$$
 (16)

where t^* denotes the time at which real change begins.

Figure 3 illustrates the behaviour on a synthetic signal with a change started at $t^* = 300$. Using k = 10, n = 30 the score D(t) remains low for all $t < t^*$, then rises sharply after $t = t^*$ and forms a peak at $t = t^* + n$ with the width of 2n timestamps. The change is considered detected when the score reaches a predefined threshold, $D(t) \ge \delta$. Additionally, for detection of onset of change, \tilde{t} is the earliest time at lift-off from zero on its way to crossing the threshold δ . Most importantly, the quality of detection depends on relative height of peaks and the variance of the score. When variance of the dissimilarity score is large, then the threshold should be large to avoid high false alarms, and thus it increases the delay in detection.

3. EXPERIMENTAL EVALUATION

3.1. Dataset

In this study, the proposed method is validated on the publicly available bearing dataset: XJTU-SY, which includes run-to-failure tests of LDKUER204 bearings. Detailed description about the testbed and experiment setup can be found in (Wang et al., 2020). Three accelerated-degradation scenarios were defined by varying rotational speed and radial load. For

each scenario, five bearings were operated until failure. The operating conditions include 2100 rpm and 12 kN, 2250 rpm and 11 kN, and 2400 rpm and 10 kN. In this experiment, vibration data were collected using two accelerometers (PCB 352C33) mounted in the vertical and horizontal directions on the bearing housing. The data were sampled at a rate of 25.6 kHz at one-minute intervals. In this study, we focus on horizontal acceleration signals. Data from the dataset bearings 2_1, 2_2, 2_5, 3_1, 3_3 and 3_4 are used in this experiment health indicator calculation.

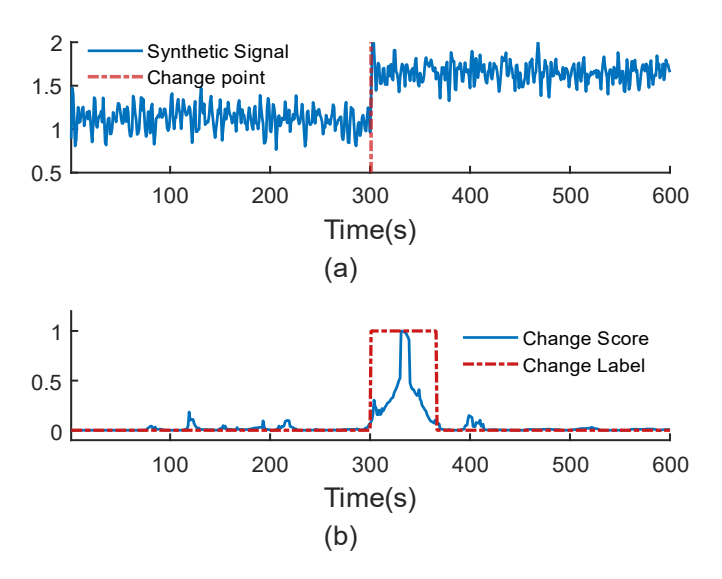


Figure 3. An Example of change detection based on direct density ratio estimation. (a) Synthetic signal with change point $t^* = 300$. (b) Calculated change score and change level.

3.2. Health Indicator Calculation

For condition monitoring of bearings, the root-mean-square (RMS) of the vibration signal is one of the most widely used HI (Yang et al., 2025). The RMS can effectively capture overall energy of the vibration signal and is sensitive to various types of degradation of bearings. Therefore, RMS is adopted for drift detection in this study. Formally, the RMS is computed over a window of m sequences of vibration samples $\{x_i\}$ at timestamp t as:

$$\mathcal{Z}(t) = \sqrt{\frac{\sum_{i}^{m} (x_i)^2}{m}} \tag{17}$$

3.3. Experimental Results and Analysis

This section presents a comprehensive evaluation of the proposed NA-RuLSIF algorithm for bearing health monitoring. Firstly, change detection performance is assessed in the context of condition monitoring and degradation. Additionally, the performance of the proposed method is evaluated in terms of early IDP detection, effective for further

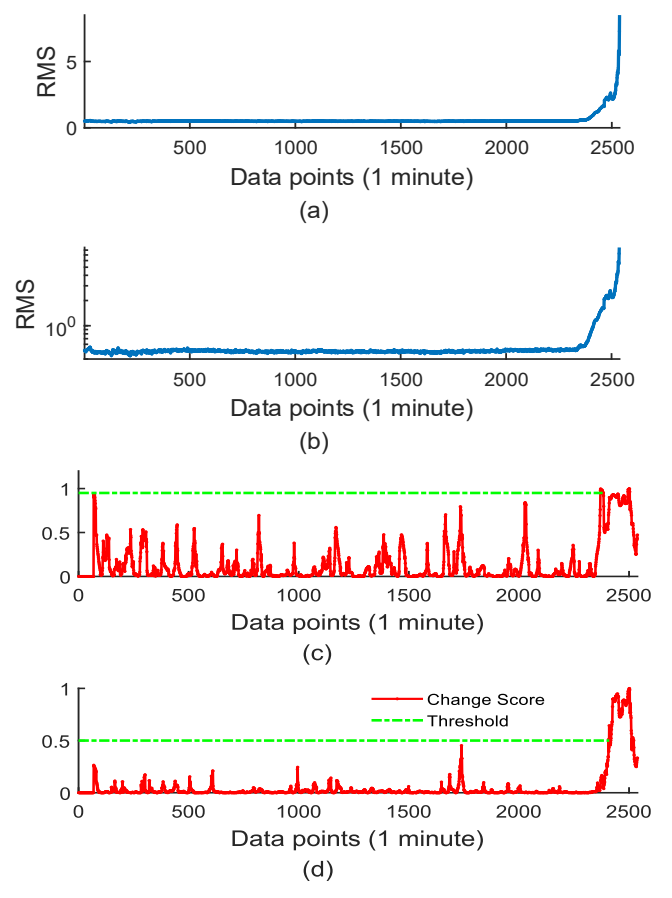


Figure 4. Run-to-failure life cycle and corresponding change score for bearing 3_1(a) HI (RMS) (b) HI (RMS) on a logarithmic scale (c) Change score obtained with RuLSIF, and (d) Change score computed with NA-RuLSIF

RUL estimation. In practice, the HI during its normal and abnormal stages is not always stable. Instead, the HI always inherently exhibits a certain degree of uncertainty and non-stationarity, which can undermine the reliability of condition monitoring algorithms. Therefore, it is worth mentioning that without any preprocessing of the HIs, a DDRE algorithm is applied to validate the robustness of the method.

To demonstrate the advantages of the proposed NA-RuLSIF algorithm over the better RuLSIF, we take account of bearing 3_1 from the XJTU-SY dataset. Figures 4(a) and 4(b) plot the raw RMS-based HI on linear and logarithmic scales, respectively. As shown in Figure 4(a), prior to data point 2342, there is no permanent drift but there are a lot of local fluctuations which are more clearly visible on the logarithm scale in Figure 4(b). After point 2342, HI shows the onset of progressive degradation leading up to failure. This onset of runaway degradation is defined as the IDP. However, the computed change score using Eq. (15) based on RuLSIF and NA-RuLSIF on raw HI is shown in Figure 4(c) and 4(d), respectively.

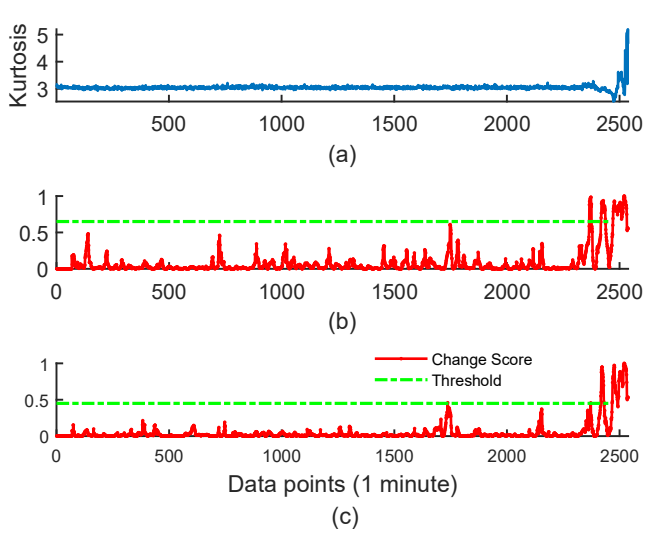


Figure 5. Run-to-failure life cycle and corresponding change score for bearing 3_1(a) HI (kurtosis) (b) Change score obtained with RuLSIF, and (c) Change score computed with NA-RuLSIF.

Although RuLSIF correctly identifies IDP, it is also sensitive to local fluctuations. Due to high variance of its change score, a higher threshold value of δ =0.9 is selected to prevent false alarms. By contrast, NA-RuLSIF computes a change IDP. This allows us to lower the threshold to δ =0.5. Therefore, NA-RuLSIF reduces detection latency and improves the reliability of degradation detection than RuLSIF. Additionally, to further demonstrate efficiency, kurtosis is used as the HI and the change score computed by RuLSIF and NA-RuLSIF are presented in Figure 5. As shown, NA-RuLSIF exhibits better performance in handling random fluctuations compared to RuLSIF for kurtosis values. Therefore, the detection threshold for NA-RuLSIF remains lower (0.4) than RuLSIF (0.7). Nevertheless, the progressive degradation trend is more distinctly captured by the RMSbased HI. Therefore, RMS-based HI is adopted throughout this study for IDP detection.

A further challenge in change detection is balancing the trade-off between detection of real degradation and falsely detecting degradation due to abrupt, local fluctuation. To determine the effectiveness of NA-RuLSIF, this study also evaluates scenarios on bearing 3_4 in Figure 6. As shown in Figure 6(b), among various degradation modes of bearings, degradation begins with run-in state, indicated by elevated RMS. After that, bearing goes through normal state until data point 1000. Then, a larger fluctuation in bearing vibration indicates a real change. Although there is no subsequent progress of the damage and bearing operates as normal, a progressive defect starts after data point 1418. In Figure 6(c)-(d), the RuLSIF exhibits significant variation while the change score of NA-RuLSIF exhibits less variation and is sensitive only when a degradation occurs. Therefore, for

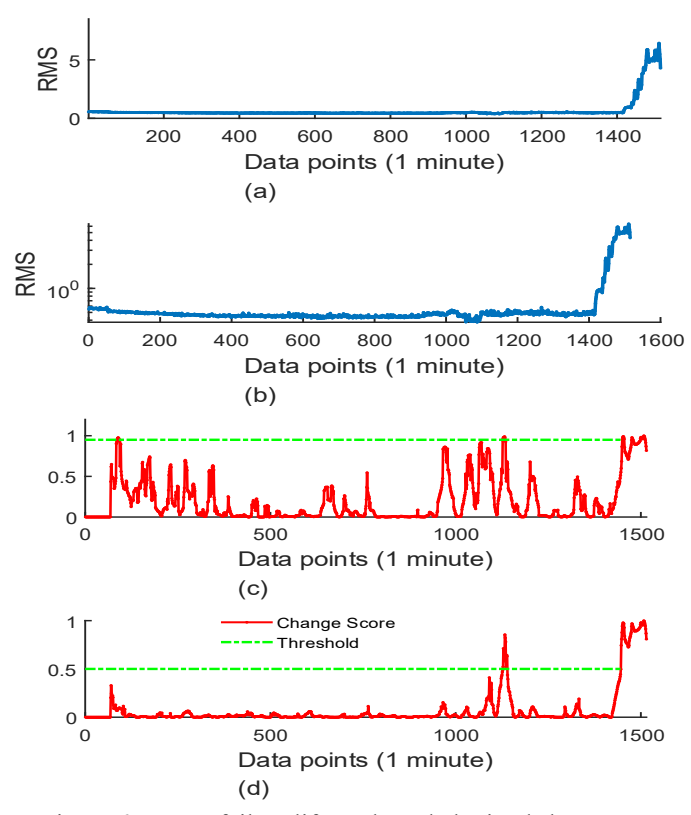


Figure 6. Run to failure life cycle and obtained change score of bearing 3_4 (a) HI (RMS) (b) HI (RMS) on a logarithmic scale (c) Change score obtained with RuLSIF and (d) Change score using NA-RuLSIF.

health monitoring NA-RuLSIF performs better and more robustly in the presence of uncertainty or random noise.

However, while the magnitude of the change score can be used to identify degradation, it does not distinguish between different types of degradation behavior, such as steady and progressive degradation. To address this, the research analyse the degradation trend to classify degradation behavior. To degradation trends, peaks values are first identified based on a predefined threshold (δ), which serves as an indicator of potential degradation. Then, the starting and ending points of these peaks are determined. Peaks with a width of less than 2n are discarded, as they are likely transient false positives. Again, peaks widths around 2n and 2n + q indicate steady degradation and local progressive degradation persistently on additional q samples respectively. Furthermore, when the right trail of peaks does not come to baseline, it indicates a progressive degradation leading to permanent failure. This scenario is illustrated in Figure 7.

Nevertheless, the selection of IDP for runaway failure is always affected by scenarios where abrupt fluctuations are followed by a return to a normal, healthy state. This abrupt

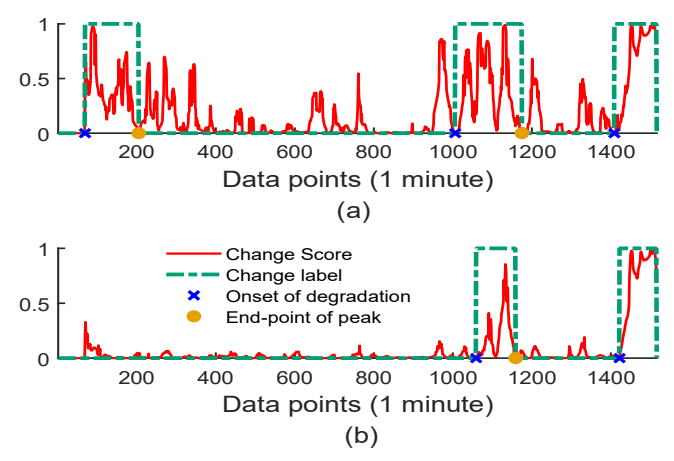


Figure 7. Change label and degradation intervals for bearing 3 4 (a) using RuLSIF (b) using NA-RuLSIF.

fluctuation can arise from various factors such as entrance of wear particles into the bearings. Therefore, performing RUL estimation from this point would disrupt the maintenance schedule and increase overall costs. Additionally, early detection of the IDP can be used as a starting point for RUL estimation. In this study, for all experiments, the parameters were set as n = 30, k = 10, and $\alpha = 0.01$ for both RuLSIF and NA-RuLSIF. Additionally, for NA-RuLSIF, the noise was generated by Eq. (12) with $\beta = 0.05$.

Therefore, using an experimental dataset, this study computes the IDP for runaway failure using RuLSIF and NA-RuLSIF methods with the results shown in Tables 1 and 2. Additionally, the table provides a comparison of the IDP positions detected by RuLSIF and NA-RuLSIF methods using performance metrics of correlation and monotonicity (Yang et al., 2025) as follows:

$$= \frac{|n \sum_{i=IDP}^{n} Z_{i} t_{i} - \sum_{i=IDP}^{n} Z_{i} \sum_{i=IDP}^{n} t_{i}|}{\sqrt{\left[n \sum_{i=IDP}^{n} Z_{i}^{2} - (\sum_{i=IDP}^{n} Z_{i})^{2}\right] \left[n \sum_{i=IDP}^{n} t_{i}^{2} - (\sum_{i=IDP}^{n} t_{i})^{2}\right]}}$$

$$M(Z) = \frac{1}{n-1} \left| \sum_{i=IDP}^{n} I((Z_{i+1}) - I(Z_i)) - \sum_{i=IDP}^{n} I((Z_i) - I(Z_{i+1})) \right|$$

In this formula, $I(\blacksquare)$ is a unit step and expressed as:

$$I(\varphi) = \begin{cases} 1, & \varphi \ge 0 \\ 0, & \varphi < 0 \end{cases}$$

After identification of IDP, performance is calculated from HI of bearings from IDP to end of life.

Table 1: IDP, Correlation and Monotonicity values obtained with RuLSIF

Bearing Name	IDP	Correlation	Monotonicity
Bearing 2_1	319	0.672	0.512
Bearing 2_2	49	0.849	0.554
Bearing 2_5	49	0.938	0.634
Bearing 3_1	1585	0.537	0.48
Bearing 3_3	48	0.45	0.18
Bearing 3_4	1409	0.966	0.736
Average		0.735	0.516

Table 2: IDP, Correlation and Monotonicity values obtained with NA-RuLSIF

Bearing Name	IDP	Correlation	Monotonicity
Bearing 2_1	458	0.99	1.0
Bearing 2_2	49	0.849	0.554
Bearing 2_5	88	0.956	0.697
Bearing 3_1	2298	0.864	0.8
Bearing 3_3	148	0.554	0.202
Bearing 3_4	1410	0.966	0.733
Average		0.863	0.664

Tables 1 and 2, list the IDP for each bearing, as determined by RuLSIF and NA-RuLSIF methods, respectively. A higher correlation and monotonicity of HI indicate better RUL estimation accuracy when RUL estimation begins from the calculated IDP. In terms of performance, NA-RuLSIF yields higher results across all six bearings than RuLSIF. This indicates that NA-RuLSIF detects IDP more precisely, from where HI shows a consistent trend until end of life.

4. CONCLUSION

This study introduces a novel DDE-based method for calculating change score from HI to detect degradation of bearings. Additionally, by exploiting both amplitude and width of the change score, this work categorizes degradation into distinct modes. Through an analysis of the behavior of change score, the optimal starting point of RUL estimation is also identified. To show the effectiveness of the proposed method, the XJTU-SY bearing dataset is used. RMS as HI is often corrupted by random noise, measurement error and the life cycle of a bearing continuously undergoing multistage degradation. The proposed NA-RuLSIF method effectively suppresses random fluctuations and reacts to real degradation more accurately than the RuLSIF method. Again, the binary partitioning of the life cycle data into two segments — normal and abnormal, is not always obvious. Consequently,

existing studies have limitations, which misidentify the true onset of degradation in scenarios where bearing vibration temporarily increases and then decreases. In the real world, an actual defect initiated by microcracks is always progressive. This research systematically categorizes these complex scenarios and reliably identifies IDP for RUL estimation. Quantitatively, the trend from IDP determined by NA-RuLSIF exhibits better consistency over various bearings in both correlation and monotonicity.

In future work, we will extend this framework to additional publicly available datasets and develop a hybrid HI based on both spatial and frequency domain for better degradation visualization. Additionally, the parameters selection and computational time complexity of NA-RuLSIF will be further investigated. Finally, by leveraging the identified IDP, we will implement and evaluate RUL estimation method through further investigations.

ACKNOWLEDGEMENT

The funding support for this work from the UKRI Strength in Places Fund Project (81801): Smart Nano-Manufacturing Corridor is gratefully acknowledged. Sanjoy Kumar Saha would like to thank Dr. Barry Dillon, Lecturer in School of Computing, Engineering, and Intelligent Systems at Ulster University, for his support.

REFERENCES

Ahmad, W., Khan, S. A., & Kim, J.-M. (2018). A Hybrid Prognostics Technique for Rolling Element Bearings Using Adaptive Predictive Models. IEEE Transactions on Industrial Electronics, 65(2), 1577–1584. https://doi.org/10.1109/TIE.2017.2733487

Bajarunas, K., Baptista, M. L., Goebel, K., & Chao, M. A. (2024). Health index estimation through integration of general knowledge with unsupervised learning. Reliability Engineering & System Safety, 251, 110352. https://doi.org/10.1016/j.ress.2024.110352

Cheng, H., Kong, X., Wang, Q., Ma, H., & Yang, S. (2022). The two-stage RUL prediction across operation conditions using deep transfer learning and insufficient degradation data. Reliability Engineering & System Safety, 225, 108581. https://doi.org/10.1016/j.ress.2022.108581

Gao, Y., Ahmad, Z., & Kim, J.-M. (2024). Fault Diagnosis of Rotating Machinery Using an Optimal Blind Deconvolution Method and Hybrid Invertible Neural Network. Sensors, 24(1), 256. https://doi.org/10.3390/s24010256

Halme, J., & Andersson, P. (2010). Rolling contact fatigue and wear fundamentals for rolling bearing diagnostics—State of the art. Proceedings of the Institution of Mechanical Engineers, Part J: Journal of Engineering Tribology, 224(4), 377–393. https://doi.org/10.1243/13506501JET656

- Huang, J., Gretton, A., Borgwardt, K., Schölkopf, B., & Smola, A. (2006). Correcting Sample Selection Bias by Unlabeled Data. Advances in Neural Information Processing Systems, 19. https://proceedings.neurips.cc/paper/2006/hash/a2186aa 7c086b46ad4e8bf81e2a3a19b-Abstract.html
- Lei, Y., Li, N., Guo, L., Li, N., Yan, T., & Lin, J. (2018). Machinery health prognostics: A systematic review from data acquisition to RUL prediction. Mechanical Systems and Signal Processing, 104, 799–834. https://doi.org/10.1016/j.ymssp.2017.11.016
- Li, N., Lei, Y., Lin, J., & Ding, S. X. (2015). An Improved Exponential Model for Predicting Remaining Useful Life of Rolling Element Bearings. IEEE Transactions on Industrial Electronics, 62(12), 7762–7773. https://doi.org/10.1109/TIE.2015.2455055
- Li, Q., Yan, C., Chen, G., Wang, H., Li, H., & Wu, L. (2022). Remaining Useful Life prediction of rolling bearings based on risk assessment and degradation state coefficient. ISA Transactions, 129, 413–428. https://doi.org/10.1016/j.isatra.2022.01.031
- Liang, X., Zuo, M. J., & Feng, Z. (2018). Dynamic modeling of gearbox faults: A review. Mechanical Systems and Signal Processing, 98, 852–876. https://doi.org/10.1016/j.ymssp.2017.05.024
- Liu, S., Yamada, M., Collier, N., & Sugiyama, M. (2013a). Change-point detection in time-series data by relative density-ratio estimation. Neural Networks, 43, 72–83. https://doi.org/10.1016/j.neunet.2013.01.012
- Liu, S., Yamada, M., Collier, N., & Sugiyama, M. (2013b). Change-point detection in time-series data by relative density-ratio estimation. Neural Networks, 43, 72–83. https://doi.org/10.1016/j.neunet.2013.01.012
- Islam, M. M., Prosvirin, A. E., & Kim, J.-M. (2021). Data-driven prognostic scheme for rolling-element bearings using a new health index and variants of least-square support vector machines. Mechanical Systems and Signal Processing, 160, 107853. https://doi.org/10.1016/j.ymssp.2021.107853
- Minhas, A. S., Kankar, P. K., Kumar, N., & Singh, S. (2021).

 Bearing fault detection and recognition methodology based on weighted multiscale entropy approach.

 Mechanical Systems and Signal Processing, 147, 107073. https://doi.org/10.1016/j.ymssp.2020.107073

- Patel, S., & Patel, S. (2024). Research progress on bearing fault diagnosis with signal processing methods for rolling element bearings. Noise & Vibration Worldwide, 55(1–2),96–112. https://doi.org/10.1177/09574565231222615
- Sugiyama, M., Suzuki, T., & Kanamori, T. (2012). Density-ratio matching under the Bregman divergence: A unified framework of density-ratio estimation. Annals of the Institute of Statistical Mathematics, 64(5), 1009–1044. https://doi.org/10.1007/s10463-011-0343-8
- Surucu, O., Gadsden, S. A., & Yawney, J. (2023). Condition Monitoring using Machine Learning: A Review of Theory, Applications, and Recent Advances. Expert Systems with Applications, 221, 119738. https://doi.org/10.1016/j.eswa.2023.119738
- Wang, B., Lei, Y., Li, N., & Li, N. (2020). A Hybrid Prognostics Approach for Estimating Remaining Useful Life of Rolling Element Bearings. IEEE Transactions on Reliability,69(1),401–412. https://doi.org/10.1109/TR.2018.2882682
- Wang, B., Lei, Y., Li, N., & Wang, W. (2021). Multiscale Convolutional Attention Network for Predicting Remaining Useful Life of Machinery. IEEE Transactions on Industrial Electronics, 68(8), 7496–7504. https://doi.org/10.1109/TIE.2020.3003649
- Yamada, M., Suzuki, T., Kanamori, T., Hachiya, H., & Sugiyama, M. (2013). Relative Density-Ratio Estimation for Robust Distribution Comparison. Neural Computation,25(5),1324–1370. https://doi.org/10.1162/NECO a 00442
- Yang, Q., Tang, B., Deng, L., & Li, Z. (2025). Adaptive early initial degradation point detection and outlier correction for bearings. Computers in Industry, 164, 104166. https://doi.org/10.1016/j.compind.2024.104166
- Zhu, J., Chen, N., & Peng, W. (2019). Estimation of Bearing Remaining Useful Life Based on Multiscale Convolutional Neural Network. IEEE Transactions on Industrial Electronics, 66(4), 3208–3216. https://doi.org/10.1109/TIE.2018.2844856